SDC-91-00057

SDC
SOLENOIDAL DETECTOR NOTES

COMMENTS ON HIGGS DETECTION IN THE WH → $l\nu\gamma\gamma$ FINAL STATE

J.F. Gunion, M. Mangano

May 1991

SDC – 91 – 00057
May, 1991

Comments on Higgs Detection in the $WH \to l\nu\gamma\gamma$ Final State*

J.F. GUNION

Department of Physics
University of California, Davis, CA 95616

M. MANGANO

Istituto Nazionale di Fisica Nucleare
Scuola Normale Superiore and Dipartimento di Fisica, Pisa, ITALY

Abstract

An intermediate mass Higgs boson may be produced in association with a W either via $q\bar{q} \to W^* \to WH$ or $gg \to t\bar{t}H \to WH+X$. Signal and background rates for detection in the final state mode $WH \to l\nu\gamma\gamma$ are investigated as a function of the rapidity coverages of the electromagnetic and muon components of the SDC detector. The impact on a number of physics issues is explored.

* Work supported in part by the U.S. Department of Energy under Contract No. DE-AT03-91ER40492.

Detection of the Standard Model Higgs boson, H, in the intermediate mass range, 70 GeV $\lesssim m_H \lesssim 2m_Z$, at a hadron collider should be regarded as an important goal. Renormalization group arguments suggest that this is precisely the range of mass that the Higgs boson should lie in if electroweak symmetry breaking can be treated perturbatively. Thus, it is crucial to assess the ability of the SDC detector operating at the SSC to probe this mass region. Until recently, the portion of this region from 70 $\lesssim m_H \lesssim$ 130 GeV has appeared to be extremely difficult to probe. Direct detection of an inclusively produced H in the two-photon decay mode[1,2] requires $\gamma\gamma$ mass resolution and jet-photon discrimination capabilities in excess of those that are likely to be achieved by the SDC detector. (See Ref. [3] and references therein.) Recently, detection in the $WH \to l\nu\gamma\gamma$ final state has been examined — backgrounds are very much smaller than in the inclusive $\gamma\gamma$ mode. The $q\bar{q} \to W^* \to WH$ process has been shown to contribute a signal in this channel that is larger than background, but with a rather small event rate at canonical $L = 10$ fb^{-1} yearly integrated luminosity. Detailed treatments including background considerations appear in Refs. [4] and [5]. A calculation of overall event rates was performed in Ref. [3]. More recently, the process $gg \to t\bar{t}H \to WHX$ was shown[6,7] to yield a much higher event rate in this channel, making detection of the H throughout the above mentioned mass range feasible at the SSC for integrated luminosity of $L = 10$ fb^{-1} provided e, μ and γ coverage extended out to about 2.5 units of rapidity. However, cost pressures may not allow for this much rapidity coverage. It is the purpose of this note to investigate the extent to which H detection in the $l\gamma\gamma$ final state will be affected by various descoping alternatives.

The options that we consider are defined by the rapidity coverage of the electromagnetic calorimetry, $y_{e,\gamma}$ and the rapidity coverage of the muon detector, y_μ. The coverage options that we explore are labelled by the pair of numbers $y_{e,\gamma} - y_\mu$. In this note we shall present results for $2.5 - 2.5$, $2.0 - 2.0$, $1.5 - 1.5$, $2.5 - 2.0$, and $2.5 - 1.5$. Standard SDC detector resolutions are employed to smear the momenta generated at the subprocess level for the detected particles. After smearing the following isolation and transverse momentum cuts are imposed:

$$p_T(l,\gamma) > 20\text{GeV}, \quad \Delta R(\gamma_1,\gamma_2) > 0.4, \quad \Delta R(l,\gamma) > 0.4. \tag{1}$$

Rapidity cuts on the l and γ's are made according to the detector coverage option chosen. The background from the $W\gamma\gamma$ and $W\gamma j$ processes has been recomputed for the various rapidity coverage options. The remaining background has been estimated at 20% of the sum of these two dominant backgrounds; this is the level found for the $2.5 - 2.5$ coverage in the study of Ref. [5]. In the case of the $t\bar{t}H$ process, we have explored top masses of $m_t = 100$, 150, and 200 GeV. Results for $l = e$ and $l = \mu$ (for a given rapidity coverage for each) are summed together in the graphs and tables to follow. For all graphs and figures we take $\sqrt{s} = 40$ TeV and integrated luminosity of $L = 10$ fb^{-1}. Finally, we shall investigate two different jet-photon discrimination factors: $R_{\gamma j} = 1 \times 10^{-3}$ and 5×10^{-4}.

We report our results in two ways. First, in order to illustrate visually the effect of the different rapidity coverage choices, we take $m_t = 150$ GeV and plot the sum

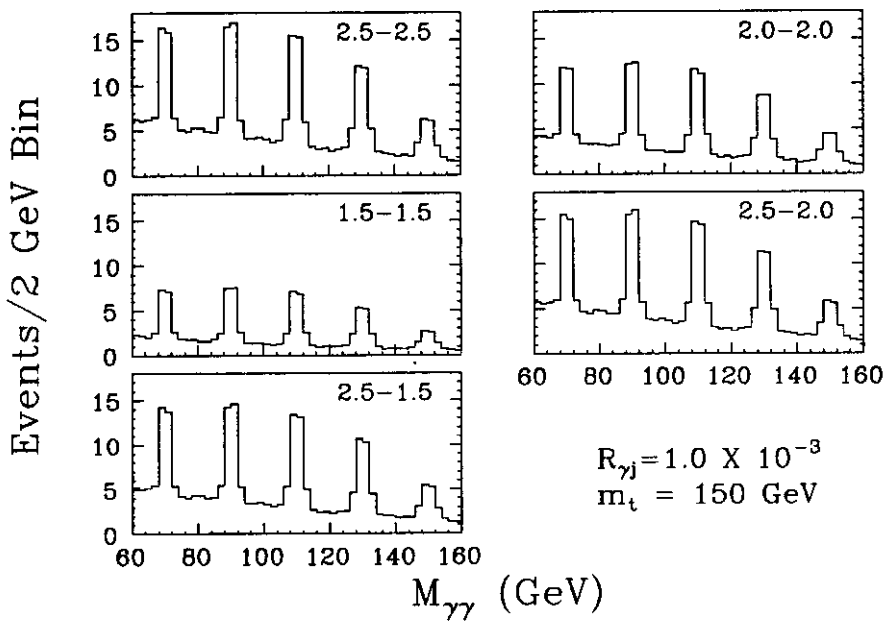

Figure 1a: Events per 2 GeV bin (for $L = 10$ fb^{-1}, $\sqrt{s} = 40$ TeV), as a function of $M_{\gamma\gamma}$. We employ $R_{\gamma j} = 1 \times 10^{-3}$ and take $m_t = 200$ GeV. The five plots are labelled by the $y_{e,\gamma} - y_\mu$ coverage options.

of the signal and background as a function of the $\gamma\gamma$ invariant mass, $M_{\gamma\gamma}$, in 2 GeV bins. Results for $R_{\gamma j} = 1 \times 10^{-3}$ appear in Fig. 1a, and for $R_{\gamma j} = 5 \times 10^{-4}$ in Fig. 1b.

In order to quantify the significance of the peaks illustrated in Fig. 1, we consider the two 2 GeV bins in $M_{\gamma\gamma}$ containing the largest number of events. (A 4 GeV total interval is probably nearly optimal; however, we have not actually attempted to optimize the interval choice.) We compute the statistical significance of the excess due to the Higgs signal in two extreme ways. At the very worst, the expected number of events in this 4 GeV interval can only be determined theoretically, and will have a statistical uncertainty given by $\sqrt{S+B}$, where S is the number of events from the Higg signal and B is the number expected if only the background processes are present. The statistical significance of the signal itself would then be given by $\sigma_- = S/\sqrt{S+B}$. However, a more optimistic viewpoint, probably not so far from reality, is that one will be able to normalize the background experimentally by looking at the entire $60 - 180$ GeV mass range in $M_{\gamma\gamma}$ outside the peak region. The shape of the background is known theoretically, and so the statistical uncertainty associated with the number of background events in the

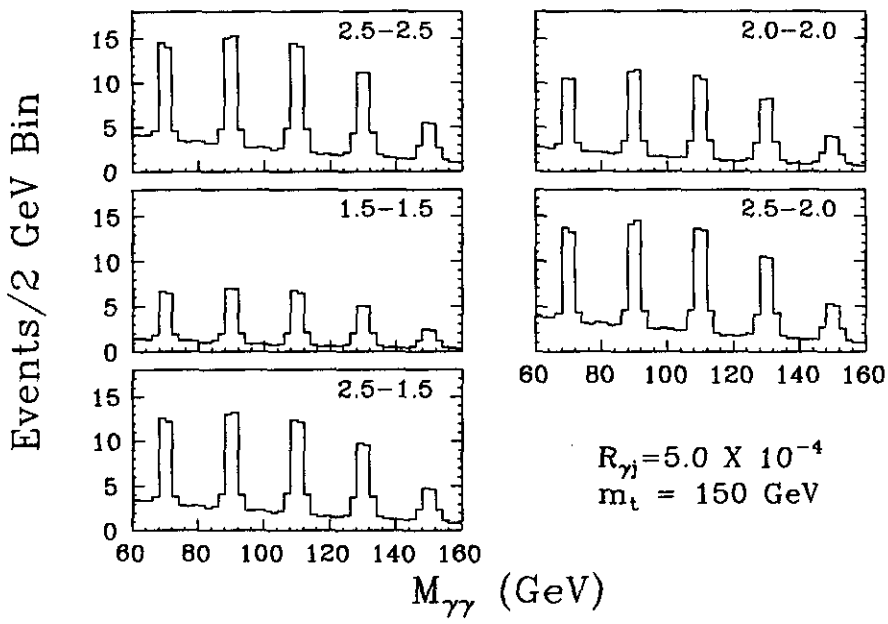

Figure 1b: Events per 2 GeV bin (for $L = 10$ fb^{-1}, $\sqrt{s} = 40$ TeV), as a function of $M_{\gamma\gamma}$. We employ $R_{\gamma j} = 5 \times 10^{-4}$ and take $m_t = 200$ GeV. The five plots are labelled by the $y_{e,\gamma} - y_\mu$ coverage options.

4 GeV interval will simply be $\sqrt{B}$, where B is the number predicted on the basis of the surrounding bins and theoretical shape. The statistical significance of the Higgs signal would then be computed as $\sigma_+ = S/\sqrt{B}$.

In Tables 1a-h we give the results for σ_- and σ_+ for a large variety of cases, including the $W^* \to WH$ process alone, and for the sum of the W^* and $t\bar{t}H$ processes computed using $m_t = 100$, 150 and 200 GeV. All results quoted in the tables are for $\sqrt{s} = 40$ TeV and $L = 10$ fb^{-1}. We now make a number of comments based on these tables. First, we note that the statistical significances for different rapidity coverages decrease in the order: $2.5-2.5$, $2.5-2.0$, $2.0-2.0 \simeq 2.5-1.5$, $1.5-1.5$, with $1.5-1.5$ being distinctly worse than the other coverage options. (For instance, if σ_- were to be the appropriate measure of statistical significance, then a 4σ peak for the $1.5-1.5$ rapidity coverage option typically requires about 50% more luminosity than for $2.0-2.0$ coverage.) From the tables it is quite clear that the combined W^* and $t\bar{t}H$ event rates make simple discovery of the Higgs boson as a 4σ peak relatively straightforward. Indeed, detection of the Higgs boson should be possible with $L = 10$ fb^{-1} for all rapidity coverages for almost all Higgs and top mass choices, provided the background can be normalized so that σ_+ is the

appropriate criterion. For the largest mass choice, $m_H = 150$ GeV, if only $1.5-1.5$ rapidity coverage is available the statistical significance of the signal falls below 4σ if one can only achieve $R_{\gamma j} = 1.0 \times 10^{-3}$. A 4σ effect as measured by σ_- can require up to $L = 33$ fb^{-1} (at $m_H = 150$ GeV) for $2.0-2.0$ or $2.5-1.5$ rapidity coverage when $R_{\gamma j} = 1.0 \times 10^{-3}$. (For $1.5-1.5$ coverage, $L = 50-55$ fb^{-1} would be needed to achieve $\sigma_- = 4$ if $m_H = 150$ GeV.)

However, simple discovery should not be the only criterion in assessing the rapidity coverage options. As discussed in Ref. [6], it is highly desirable to be able to measure the W^* and $t\bar{t}H$ processes separately in order to determine the ratio of the HW^+W^- and $Ht\bar{t}$ couplings. To do so, one must measure the W^* subprocess separately by imposing anti-tagging cuts that discriminate against the extra jets and/or leptons present for the $t\bar{t}H$ process, see Ref. [6]. A completely precise study of this issue requires a study of how the backgrounds behave under such anti-tagging cuts. However, the main backgrounds, from $W\gamma\gamma$ and $W\gamma j$, will be little affected by these extra cuts. And, of course, the number of events from the W^* process of interest should not be reduced significantly by the anti-tagging cuts. In addition, we will assume that the number of events from the $t\bar{t}H$ subprocess can either be reduced by appropriate anti-tagging to a relatively negligible level or be rather precisely normalized using the uncut data. We can then compute the statistical significance of the W^* signal as either (pessimistically) $\sigma_-^{W^*} = S^{W^*}/\sqrt{S^{W^*}+B}$ or (optimistically) $\sigma_+^{W^*} = S^{W^*}/\sqrt{B}$.

From the Tables 1a and 1e we see that a 4σ effect in $\sigma_+^{W^*}$ requires of order $L = 110-160$ fb^{-1} for $70 \lesssim m_H \lesssim 130$ GeV when $2.0-2.0$ rapidity coverage is available, but as much as $L = 250$ fb^{-1} if only $1.5-1.5$ coverage is in place. For $m_H \gtrsim 150$ GeV, separation of the W^* process would require enormous luminosity. However, for m_H values above about 135 GeV observation of the Higgs boson in the $H \to ZZ^* \to l^+l^-l^+l^-$ channel will almost certainly be possible and will allow a direct measurement of the HZZ coupling. One will then be able to compute the W-loop and t-loop contributions to the $H \to \gamma\gamma$ decay width in the Standard Model, and thereby determine the expected rate for $t\bar{t}H \to l\gamma\gamma X$. This can be compared to the observed rate in order to assess the correctness of the Standard Model. However, by $m_H = 170$ GeV even the number of $t\bar{t}H \to l\gamma\gamma X$ events will reach an undetectable level — $\lesssim 1$ event is obtained for $L = 10$ fb^{-1}. This is due to the rapid decline in the $H \to \gamma\gamma$ branching ratio for $m_H \gtrsim 150$ GeV. The maximum region of overlap where direct observation of both $t\bar{t}H \to l\gamma\gamma X$ and $H \to 4l$ is possible extends from about 130 GeV to around 160 GeV, assuming $L = 100$ fb^{-1} and any of the top three rapidity coverage options. The $1.5-1.5$ coverage option would shrink this overlap interval significantly.

Our overall conclusion regarding the descoping alternatives is easily stated. Discovery of *and* the ability to study the couplings of an intermediate mass Standard Model Higgs boson using the signal from $WHX \to l\gamma\gamma X$ final states will only be severely impacted by the $y_{e,\gamma} = 1.5 - y_\mu = 1.5$ rapidity coverage option. In particular, the $2.5-1.5$ and $2.0-2.0$ options are highly preferable.

Acknowledgements

We would like to thank our SDC colleagues for stimulating our interest in this study.

REFERENCES

1. J.F. Gunion, P. Kalyniak, M. Soldate, and P. Galison, *Phys. Rev.* **D34** (1986) 101.
2. J.F. Gunion, G.L. Kane, and J. Wudka, *Nucl. Phys.* **B299** (1988) 231.
3. J.F. Gunion, G.L. Kane *et al.*, 'Overview and Recent Progress in Higgs Boson Physics at the SSC', to appear in *Proceedings of the 1990 Snowmass Summer Study on "Research Directions for the Decade"*, preprint PRINT-91-0010 (1990).
4. R. Kleiss, Z. Kunszt, and J. Stirling, preprint DTP-90-54.
5. M. Mangano, SDC Collaboration Note SSC-SDC-90-00113.
6. J.F. Gunion, preprint UCD-91-2 (January, 1991), to appear in *Phys. Lett.* **B**.
7. W. J. Marciano and F.E. Paige, preprint BNL-45805 (February, 1991).

m_H	$y_{e,\gamma} - y_\mu$	S	$S+B$	σ_-	σ_+
70	2.5 − 2.5	4.3	15.5	1.1	1.3
	2.0 − 2.0	3.2	10.6	1.0	1.2
	1.5 − 1.5	2.0	6.1	0.8	1.0
	2.5 − 2.0	4.1	14.5	1.1	1.3
	2.5 − 1.5	3.7	13.1	1.0	1.2
90	2.5 − 2.5	4.6	13.6	1.3	1.5
	2.0 − 2.0	3.2	9.0	1.1	1.3
	1.5 − 1.5	2.0	5.0	0.9	1.1
	2.5 − 2.0	4.3	12.6	1.2	1.5
	2.5 − 1.5	4.0	11.4	1.2	1.4
110	2.5 − 2.5	4.0	10.7	1.2	1.6
	2.0 − 2.0	2.8	7.1	1.1	1.4
	1.5 − 1.5	1.6	3.7	0.8	1.1
	2.5 − 2.0	3.8	10.0	1.2	1.5
	2.5 − 1.5	3.5	9.0	1.2	1.5
130	2.5 − 2.5	2.9	8.2	1.0	1.2
	2.0 − 2.0	2.0	5.3	0.9	1.1
	1.5 − 1.5	1.2	2.8	0.7	1.0
	2.5 − 2.0	2.7	7.6	1.0	1.2
	2.5 − 1.5	2.5	6.9	0.9	1.2
150	2.5 − 2.5	1.1	4.9	0.5	0.6
	2.0 − 2.0	0.8	3.2	0.4	0.5
	1.5 − 1.5	0.5	1.7	0.4	0.4
	2.5 − 2.0	1.1	4.6	0.5	0.6
	2.5 − 1.5	1.0	4.2	0.5	0.5

Table 1a: $R_{\gamma j} = 1.0 \times 10^{-3}$, $W^* \to WH$ only

m_H	$y_{e,\gamma} - y_\mu$	S	$S+B$	σ_-	σ_+
	2.5 – 2.5	17.7	28.9	3.3	5.3
	2.0 – 2.0	13.6	21.1	3.0	5.0
70	1.5 – 1.5	8.9	13.1	2.5	4.4
	2.5 – 2.0	16.8	27.2	3.2	5.2
	2.5 – 1.5	15.5	24.9	3.1	5.1
	2.5 – 2.5	21.4	30.4	3.9	7.1
	2.0 – 2.0	16.0	21.8	3.4	6.7
90	1.5 – 1.5	10.4	13.4	2.8	6.0
	2.5 – 2.0	20.2	28.5	3.8	7.0
	2.5 – 1.5	18.9	26.3	3.7	6.9
	2.5 – 2.5	20.1	26.8	3.9	7.8
	2.0 – 2.0	15.3	19.6	3.5	7.4
110	1.5 – 1.5	9.3	11.4	2.8	6.4
	2.5 – 2.0	19.2	25.4	3.8	7.7
	2.5 – 1.5	17.5	23.1	3.6	7.4
	2.5 – 2.5	16.6	21.9	3.5	7.2
	2.0 – 2.0	12.0	15.2	3.1	6.7
130	1.5 – 1.5	7.7	9.3	2.5	6.2
	2.5 – 2.0	15.4	20.2	3.4	7.0
	2.5 – 1.5	14.1	18.5	3.3	6.7
	2.5 – 2.5	9.5	13.3	2.6	4.9
	2.0 – 2.0	6.6	9.0	2.2	4.2
150	1.5 – 1.5	3.9	5.1	1.7	3.4
	2.5 – 2.0	9.0	12.5	2.5	4.8
	2.5 – 1.5	8.2	11.5	2.4	4.6

Table 1b: $R_{\gamma j} = 1.0 \times 10^{-3}$, $W^* \to WH + t\bar{t}H \to WHX$, $m_t = 100$ GeV

m_H	$y_{e,\gamma} - y_\mu$	S	$S+B$	σ_-	σ_+
70	2.5 – 2.5	21.6	32.8	3.8	6.5
	2.0 – 2.0	16.2	23.7	3.3	5.9
	1.5 – 1.5	10.6	14.8	2.8	5.2
	2.5 – 2.0	20.6	30.9	3.7	6.4
	2.5 – 1.5	18.9	28.3	3.6	6.2
90	2.5 – 2.5	24.1	33.1	4.2	8.0
	2.0 – 2.0	18.7	24.4	3.8	7.8
	1.5 – 1.5	12.1	15.1	3.1	7.0
	2.5 – 2.0	22.9	31.2	4.1	8.0
	2.5 – 1.5	21.1	28.6	4.0	7.7
110	2.5 – 2.5	24.5	31.2	4.4	9.5
	2.0 – 2.0	18.6	22.9	3.9	9.0
	1.5 – 1.5	12.0	14.1	3.2	8.2
	2.5 – 2.0	23.2	29.4	4.3	9.3
	2.5 – 1.5	21.2	26.8	4.1	9.0
130	2.5 – 2.5	18.3	23.6	3.8	8.0
	2.0 – 2.0	13.9	17.1	3.4	7.7
	1.5 – 1.5	9.1	10.7	2.8	7.3
	2.5 – 2.0	17.4	22.3	3.7	7.9
	2.5 – 1.5	16.2	20.7	3.6	7.7
150	2.5 – 2.5	8.6	12.4	2.4	4.4
	2.0 – 2.0	6.6	9.0	2.2	4.2
	1.5 – 1.5	4.1	5.4	1.8	3.7
	2.5 – 2.0	8.3	11.8	2.4	4.4
	2.5 – 1.5	7.6	10.8	2.3	4.2

Table 1c: $R_{\gamma j} = 1.0 \times 10^{-3}$, $W^* \to WH + t\bar{t}H \to WHX$, $m_t = 150$ GeV

m_H	$y_{e,\gamma} - y_\mu$	S	$S+B$	σ_-	σ_+
70	2.5 − 2.5	22.0	33.2	3.8	6.6
	2.0 − 2.0	17.3	24.8	3.5	6.3
	1.5 − 1.5	11.4	15.5	2.9	5.6
	2.5 − 2.0	21.1	31.5	3.8	6.5
	2.5 − 1.5	19.3	28.7	3.6	6.3
90	2.5 − 2.5	25.7	34.7	4.4	8.6
	2.0 − 2.0	19.9	25.6	3.9	8.3
	1.5 − 1.5	12.9	15.9	3.2	7.4
	2.5 − 2.0	24.5	32.8	4.3	8.5
	2.5 − 1.5	22.8	30.3	4.2	8.4
110	2.5 − 2.5	25.6	32.3	4.5	9.9
	2.0 − 2.0	20.0	24.3	4.1	9.6
	1.5 − 1.5	12.8	14.9	3.3	8.8
	2.5 − 2.0	24.3	30.5	4.4	9.8
	2.5 − 1.5	22.4	28.0	4.2	9.5
130	2.5 − 2.5	21.1	26.4	4.1	9.2
	2.0 − 2.0	16.5	19.7	3.7	9.2
	1.5 − 1.5	10.3	11.9	3.0	8.2
	2.5 − 2.0	20.2	25.1	4.0	9.1
	2.5 − 1.5	18.8	23.3	3.9	9.0
150	2.5 − 2.5	8.9	12.7	2.5	4.6
	2.0 − 2.0	6.8	9.2	2.2	4.4
	1.5 − 1.5	4.3	5.6	1.8	3.9
	2.5 − 2.0	8.5	12.0	2.5	4.5
	2.5 − 1.5	7.8	11.0	2.4	4.4

Table 1d: $R_{\gamma j} = 1.0 \times 10^{-3}$, $W^* \to WH + t\bar{t}H \to WHX$, $m_t = 200$ GeV

m_H	$y_{e,\gamma} - y_\mu$	S	$S+B$	σ_-	σ_+
70	2.5 − 2.5	4.3	11.8	1.3	1.6
	2.0 − 2.0	3.2	8.1	1.1	1.4
	1.5 − 1.5	2.0	4.7	0.9	1.2
	2.5 − 2.0	4.1	11.0	1.2	1.6
	2.5 − 1.5	3.7	9.9	1.2	1.5
90	2.5 − 2.5	4.6	10.5	1.4	1.9
	2.0 − 2.0	3.2	7.0	1.2	1.7
	1.5 − 1.5	2.0	3.9	1.0	1.4
	2.5 − 2.0	4.3	9.8	1.4	1.9
	2.5 − 1.5	4.0	8.8	1.3	1.8
110	2.5 − 2.5	4.0	8.4	1.4	1.9
	2.0 − 2.0	2.8	5.6	1.2	1.7
	1.5 − 1.5	1.6	3.0	1.0	1.4
	2.5 − 2.0	3.8	7.8	1.4	1.9
	2.5 − 1.5	3.5	7.1	1.3	1.8
130	2.5 − 2.5	2.9	6.4	1.1	1.5
	2.0 − 2.0	2.0	4.1	1.0	1.4
	1.5 − 1.5	1.2	2.2	0.8	1.2
	2.5 − 2.0	2.7	5.9	1.1	1.5
	2.5 − 1.5	2.5	5.4	1.1	1.4
150	2.5 − 2.5	1.1	3.6	0.6	0.7
	2.0 − 2.0	0.8	2.3	0.5	0.6
	1.5 − 1.5	0.5	1.2	0.4	0.5
	2.5 − 2.0	1.1	3.3	0.6	0.7
	2.5 − 1.5	1.0	3.0	0.6	0.7

Table 1e: $R_{\gamma j} = 5.0 \times 10^{-4}$, $W^* \to WH$ only

m_H	$y_{e,\gamma} - y_\mu$	S	$S+B$	σ_-	σ_+
70	2.5 – 2.5	17.7	25.2	3.5	6.5
	2.0 – 2.0	13.6	18.5	3.2	6.1
	1.5 – 1.5	8.9	11.6	2.6	5.4
	2.5 – 2.0	16.8	23.7	3.5	6.4
	2.5 – 1.5	15.5	21.7	3.3	6.2
90	2.5 – 2.5	21.4	27.2	4.1	8.8
	2.0 – 2.0	16.0	19.7	3.6	8.3
	1.5 – 1.5	10.4	12.3	3.0	7.5
	2.5 – 2.0	20.2	25.6	4.0	8.7
	2.5 – 1.5	18.9	23.7	3.9	8.6
110	2.5 – 2.5	20.1	24.5	4.1	9.6
	2.0 – 2.0	15.3	18.0	3.6	9.2
	1.5 – 1.5	9.3	10.6	2.9	8.1
	2.5 – 2.0	19.2	23.3	4.0	9.6
	2.5 – 1.5	17.5	21.2	3.8	9.2
130	2.5 – 2.5	16.6	20.2	3.7	8.8
	2.0 – 2.0	12.0	14.1	3.2	8.3
	1.5 – 1.5	7.7	8.8	2.6	7.7
	2.5 – 2.0	15.4	18.6	3.6	8.5
	2.5 – 1.5	14.1	17.0	3.4	8.2
150	2.5 – 2.5	9.5	12.0	2.7	6.1
	2.0 – 2.0	6.6	8.1	2.3	5.3
	1.5 – 1.5	3.9	4.6	1.8	4.4
	2.5 – 2.0	9.0	11.2	2.7	6.0
	2.5 – 1.5	8.2	10.3	2.6	5.7

Table 1f: $R_{\gamma j} = 5.0 \times 10^{-4}$, $W^* \to WH + t\bar{t}H \to WHX$, $m_t = 100$ GeV

m_H	$y_{e,\gamma} - y_\mu$	S	$S+B$	σ_-	σ_+
70	2.5 – 2.5	21.6	29.1	4.0	7.9
	2.0 – 2.0	16.2	21.1	3.5	7.3
	1.5 – 1.5	10.6	13.3	2.9	6.4
	2.5 – 2.0	20.6	27.5	3.9	7.8
	2.5 – 1.5	18.9	25.1	3.8	7.6
90	2.5 – 2.5	24.1	30.0	4.4	10.0
	2.0 – 2.0	18.7	22.4	3.9	9.7
	1.5 – 1.5	12.1	14.0	3.2	8.7
	2.5 – 2.0	22.9	28.3	4.3	9.9
	2.5 – 1.5	21.1	26.0	4.1	9.6
110	2.5 – 2.5	24.5	28.9	4.6	11.7
	2.0 – 2.0	18.6	21.4	4.0	11.2
	1.5 – 1.5	12.0	13.3	3.3	10.4
	2.5 – 2.0	23.2	27.3	4.4	11.5
	2.5 – 1.5	21.2	24.8	4.3	11.1
130	2.5 – 2.5	18.3	21.9	3.9	9.8
	2.0 – 2.0	13.9	16.0	3.5	9.6
	1.5 – 1.5	9.1	10.1	2.9	9.0
	2.5 – 2.0	17.4	20.6	3.8	9.7
	2.5 – 1.5	16.2	19.2	3.7	9.5
150	2.5 – 2.5	8.6	11.1	2.6	5.5
	2.0 – 2.0	6.6	8.1	2.3	5.3
	1.5 – 1.5	4.1	4.9	1.9	4.6
	2.5 – 2.0	8.3	10.5	2.5	5.5
	2.5 – 1.5	7.6	9.7	2.4	5.3

Table 1g: $R_{\gamma j} = 5.0 \times 10^{-4}$, $W^* \to WH + t\bar{t}H \to WHX$, $m_t = 150$ GeV

m_H	$y_{e,\gamma} - y_\mu$	S	$S+B$	σ_-	σ_+
	2.5 − 2.5	22.0	29.5	4.1	8.1
	2.0 − 2.0	17.3	22.2	3.7	7.8
70	1.5 − 1.5	11.4	14.1	3.0	6.9
	2.5 − 2.0	21.1	28.0	4.0	8.0
	2.5 − 1.5	19.3	25.5	3.8	7.7
	2.5 − 2.5	25.7	31.6	4.6	10.6
	2.0 − 2.0	19.9	23.6	4.1	10.3
90	1.5 − 1.5	12.9	14.9	3.4	9.3
	2.5 − 2.0	24.5	30.0	4.5	10.6
	2.5 − 1.5	22.8	27.7	4.3	10.4
	2.5 − 2.5	25.6	30.0	4.7	12.2
	2.0 − 2.0	20.0	22.7	4.2	12.0
110	1.5 − 1.5	12.8	14.1	3.4	11.1
	2.5 − 2.0	24.3	28.3	4.6	12.1
	2.5 − 1.5	22.4	26.0	4.4	11.8
	2.5 − 2.5	21.1	24.6	4.3	11.2
	2.0 − 2.0	16.5	18.6	3.8	11.3
130	1.5 − 1.5	10.3	11.3	3.1	10.2
	2.5 − 2.0	20.2	23.4	4.2	11.2
	2.5 − 1.5	18.8	21.8	4.0	11.0
	2.5 − 2.5	8.9	11.4	2.6	5.7
	2.0 − 2.0	6.8	8.3	2.4	5.5
150	1.5 − 1.5	4.3	5.1	1.9	4.9
	2.5 − 2.0	8.5	10.8	2.6	5.6
	2.5 − 1.5	7.8	9.9	2.5	5.4

Table 1h: $R_{\gamma j} = 5.0 \times 10^{-4}$, $W^* \to WH + t\bar{t}H \to WHX$, $m_t = 200$ GeV